

pubs.acs.org/acsapm Article

Universality in Solution Properties of Polymers in Ionic Liquids

Ryan Sayko, Michael Jacobs, and Andrey V. Dobrynin*



Cite This: ACS Appl. Polym. Mater. 2022, 4, 1966-1973



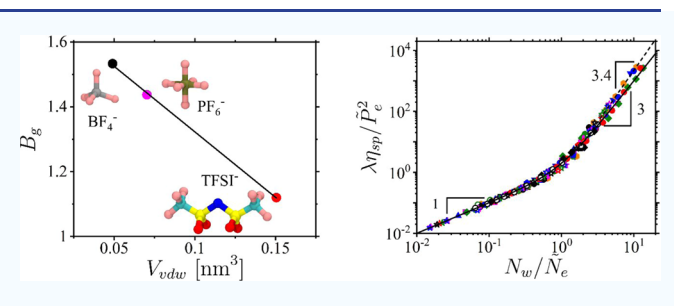
ACCESS I

Metrics & More

Article Recommendations

SI Supporting Information

ABSTRACT: Knowledge of the interaction parameters for polymers in different solvents is crucial for exploring the viscoelastic properties and processing capabilities of polymer solutions. Here, we apply a scaling theory of semidilute polymer solutions to quantify the solution properties of cellulose, poly(ethylene oxide), poly(methyl methacrylate), and poly-(acrylonitrile-co-itaconic acid) in different ionic liquids. The starting point of our approach is a scaling relationship between the solution correlation length $\xi = lg^{\nu}/B$ and the number of repeat units g in a correlation blob for polymers with a repeat unit



projection length l, chain segment fractal dimension $1/\nu$, and the corresponding interaction parameter B describing polymer—solvent affinity and assuming values B_g , $B_{\rm th}$, and 1 in different solution regimes. In the framework of this approach, we obtain crossover concentrations to the semidilute solution regime, c^* , the solution regime of overlapping thermal blobs, $c_{\rm th}$, and the concentrated solution regime, c^* . The method takes advantage of the linear relationship of the specific viscosity $\eta_{\rm sp}$ with the number of correlation blobs per chain $N_{\rm w}/g$ in the unentangled Rouse regime for polymers with a weight-average degree of polymerization $N_{\rm w}$. The application of our approach to entangled solutions provides the chain packing number, $P_{\rm e}$, and completes the set of parameters $\{B_g, B_{\rm th}, {\rm and} \ P_{\rm e}\}$ that uniquely describes the static and dynamic solution properties for a given polymer/solvent pair. This approach also allows us to identify a trend relating the B_g parameter to the van der Waals volume of the ionic liquid anion, analogous to the Hofmeister series, and to obtain the temperature and solvent type dependence of the polymer excluded volume and Kuhn length.

KEYWORDS: polymers, ionic liquids, scaling, polymer solutions, solution viscosity

■ INTRODUCTION

Ionic liquids are made of asymmetric cation/anion pairs and can remain in a liquid state over a wide temperature range. The properties of ionic liquids can be fine-tuned by a judicial choice of cations and anions to target polymer-specific applications (see for review¹⁻⁴). For currently known ionic liquids, there are approximately 1012 different pair combinations (with ternary mixtures, we have access to 10¹⁸ possible combinations), which allows for broad variations in ionic liquid properties.5 The huge number of possible combinations has prompted research into understanding the relationship between the chemical structures of ionic liquid components and their properties as solvents.⁶⁻¹³ Furthermore, the low volatility, nonflammability, thermal and chemical stability, tunable solvation, and conductivity of ionic liquids have stimulated their use as a "green solvent" replacement for volatile organic solvents in polymerization, polymer processing and separation, and as supporting media in electrolytic processes. 14,15

However, in order to take full advantage of the promise offered by ionic liquids, we need an efficient and simple method for the characterization of the properties of polymers in such solutions. Recently, we have developed an approach based on the scaling model of semidilute polymer solutions that has allowed us to obtain polymer—solvent interaction

parameters and quantify their static and dynamic properties from the analysis of concentration dependence of the solution specific viscosity. This method has been successful in describing the solution properties of neutral polymers, 16 polyelectrolytes, 17,18 and biomacromolecules. 19 Building on this success, we apply this approach to characterize solutions of natural and synthetic polymers in ionic liquids. Specifically, we obtain polymer-ionic liquid interaction parameters responsible for the chain's statistics at different length scales, crossover concentrations into different solution regimes, and a packing parameter describing chain entanglements. The obtained interaction parameters for the solutions of polymers in ionic liquids are compared with those for polymers in aqueous solutions when available. We also demonstrate a dependence of the solvent quality on the size of the anions for poly(ethylene oxide) in ionic liquids with 1-butyl-3-methylimidazolium cations, similar to the Hofmeister series. 20-24 To illustrate the universality of our approach, we represent

Received: December 13, 2021 Accepted: February 4, 2022 Published: February 17, 2022





solution viscosity data in terms of a ratio $N_{\rm w}/N_{\rm e}$ of the weight-average degree of polymerization, $N_{\rm w}$, and the concentration-dependent degree of polymerization between entanglements, $N_{\rm e}$.

The rest of the paper is organized as follows. We begin with a brief overview of the scaling approach used in our analysis of the solution properties of polymers in ionic liquids. This is followed by an illustration of the method on the viscosity data of cellulose in ionic liquids 1-ethyl-3-methylimidazolium methylphosphonate ([EMIm][P(OCH₃)(H)O₂]), 1-butyl-3-methylimidazolium chloride ([BMIm][Cl]), 1-allyl-3-methylimidazolium formate ([AMIm][COOH]), and 1-ethyl-3-methylimidazolium acetate ([EMIm][Ac]). Using the obtained interaction parameters for cellulose, poly(ethylene oxide) (PEO), poly(methyl methacrylate) (PMMA), and poly-(acrylonitrile-co-itaconic acid) (P(AN-co-IA)) in ionic liquids, we construct a diagram of states of polymers in ionic liquids and obtain the temperature and solvent type dependence of the chain Kuhn length and excluded volume.

METHOD

In our analysis of experimental data, we use a scaling model of semidilute polymer solutions which assumes the existence of a characteristic length—the solution correlation length ξ —beyond which all interactions are screened and the chain's statistics is that of an ideal chain of correlation blobs with size ξ . However, on the length scales smaller than the solution correlation length, the polymer statistics is controlled by specific polymer—solvent interactions. This provides the following relationship between the solution correlation length ξ and the number of repeat units g in it

$$\xi = \lg^{\nu}/B \tag{1}$$

where l is the repeat unit projection length, ν is the scaling exponent, and the B-parameter encapsulates the details of the polymer—solvent interactions. In the different solution regimes, depending on the repeat unit concentration, the scaling exponent ν is equal to 0.588, 0.5, and 1, and the B-parameter takes on the values B_g , B_{th} , and 1. This reflects a hierarchical organization of the polymer chain in semidilute solutions as illustrated in Figure 1a. In particular, the parameter B_g characterizes the chain properties on length scales larger than the thermal blob size, D_{th} , and is defined as

$$B_{g} = l(lb)^{3\nu - 2} v^{1 - 2\nu}$$
 (2)

where ν is the repeat unit excluded volume, b is the Kuhn length, and the exponent $\nu=0.588$. This definition of $B_{\rm g}$ follows from the Flory expression for the chain size in a good solvent. Note that the $B_{\rm g}$ -parameter quantifies the solvent quality for the polymer backbone.

Within a thermal blob, on length scales, $b < r \le D_{\rm th}$, sections of the chain are ideal with exponent $\nu = 0.5$ and

$$B_{\rm th} = (l/b)^{0.5} \tag{3}$$

The B_{th} -parameter characterizes chain flexibility and decreases with an increasing number of repeat units per Kuhn length.

Finally, on length scales smaller than the Kuhn length, the chain segments are rod-like, which corresponds to B=1 and $\nu=1$

In a θ solvent for the polymer backbone, B assumes values of $B_{\rm th}$ and 1, where the exponent ν is 0.5 and 1, respectively.

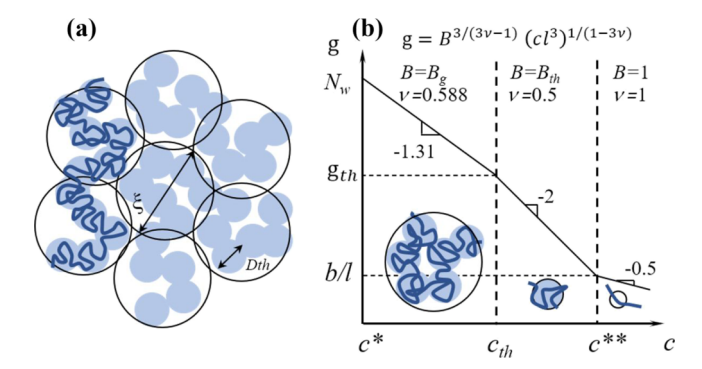


Figure 1. (a) Schematic representation of hierarchy of length scales in semidilute polymer solutions in a good solvent. Correlation blobs with size ξ contain thermal blobs with size $D_{\rm th}$. (b) Concentration dependence of the number of monomers g per correlation blob. c^* —chain overlap concentration, $c_{\rm th}$ —thermal blob overlap concentration, and c^{**} —crossover concentration to the concentrated solution regime. Insets show the chain structure on the length scales of correlation blobs. Logarithmic scales. Adapted from ref 16. Copyright ACS 2021.

Taking into account the space-filling condition of the correlation blobs such that the repeat unit concentration inside the blobs is equal to the solution concentration

$$c = g/\xi^3 \tag{4}$$

and using eq 1, we obtain the correlation length ξ and the number of repeat units g per correlation blob as functions of the dimensionless concentration of repeat units $\varphi = cl^3$

$$\xi = lB^{1/(3\nu - 1)} \varphi^{\nu/(1 - 3\nu)} \tag{5a}$$

$$g = B^{3/(3\nu - 1)} \varphi^{1/(1 - 3\nu)} \tag{5b}$$

Figure 1b shows the concentration dependence of the number of repeat units per correlation blob in different solution regimes. The corresponding crossover concentrations between solution regimes are c^* —chain overlap concentration, $c_{\rm th}$ —crossover concentration to a solution of overlapping thermal blobs, and c^{**} —crossover concentration to the concentrated polymer solution regime. The polymer overlap concentration c^* is determined by taking eq 5b in the limit of $g = N_{\rm w}$

$$c^*l^3 = B^3 N_{\rm w}^{1-3\nu} \tag{6}$$

where $\nu=0.588$ and $B=B_{\rm g}$ for a good solvent, and $\nu=0.5$ and $B=B_{\rm th}$ in the case of a θ solvent. Note that here we use the weight-average degree of polymerization $N_{\rm w}$ to determine the B-parameter at $c=c^*$. By equating eq Sb in the regimes corresponding to the parameters $B_{\rm g}$ and $B_{\rm th}$ at the thermal blob overlap concentration $c_{\rm th}$, one obtains

$$c_{\rm th}l^3 = B_{\rm th}^3 (B_{\rm th}/B_{\rm g})^{1/(2\nu-1)}$$
 (7)

Finally, the crossover concentration to the concentrated solution regime occurs at

$$c^{**}l^3 = B_{\text{th}}^4 = l^2/b^2 \tag{8}$$

for which the correlation length is equal to the Kuhn length, $\xi(c^{**}) = b$. The Kuhn length and repeat unit excluded volume have the following explicit forms in terms of $B_{\rm th}$ and $c_{\rm th}$

$$b = l/B_{\rm th}^{2} \tag{9a}$$

Polymers

Ionic Liquid Components

Cations Anions 1-allyl-3-methylimidazolium 1-ethyl-3-methylimidazolium (AMIm) (EMÍm) Tetrafluoroborate Methylphosphonate Hexafluorophosphate (BF_4) $(P(OCH_3)(H)O_2)$ (PF_6) 1-butyl-3-methylimidazolium (BMIm) Cl-Chloride Acetate bis(trifluoromethylsulfonyl)imide Formate (CI) (COOH) (TFSI) (Ac)

Figure 2. Summary of studied polymers and ionic liquid components.

$$v = bl^2 c_{th} / c^{**} \tag{9b}$$

It is important to point out that the value of the $B_{\rm th}$ -parameter is required for the calculations of c^{**} (eq 8) and the Kuhn length (eq 9a). However, in order to obtain the excluded volume parameter (eq 9b), the values of both $B_{\rm g}$ and $B_{\rm th}$ must be known.

Our approach to obtaining the *B*-parameters from the solution viscosity as a function of polymer concentration is based on the linear dependence of the specific viscosity on the number of correlation blobs per chain in the Rouse (unentangled) solution regime^{26,27}

$$\eta_{\rm sp} = N_{\rm w}/g \tag{10}$$

Therefore, according to eq 5b, we can use a normalized specific viscosity $\eta_{\rm sp}/N_{\rm w}(cl^3)^{1/(3\nu-1)}$ to find the plateau or minimum value $C_{\rm p}$ corresponding to the different solution concentration regimes and obtain the values of the *B*-parameters as

$$B = C_{\rm p}^{1/3-\nu} \tag{11}$$

With increasing solution concentration, the chains of blobs begin to entangle. The solution specific viscosity $\eta_{\rm sp}$ has the following crossover expression to the entangled semidilute solution regime

$$\eta_{\rm sp} = N_{\rm w} \left(1 + \left(\frac{N_{\rm w}}{\tilde{N}_{\rm e}} \right)^2 \right) \left\{ g^{-1}, \text{ for } c \le c^{**} \right\}$$

$$\left(cbl^2, \text{ for } c^{**} < c \right) (12)$$

where $\tilde{N}_{\rm e}$ is the number of repeat units per entanglement strand. The accent character "~" is used to indicate that the system polydispersity is included in the definition of the number of repeat units per entanglement strand $N_{\rm e}$. The concentration dependence of $\tilde{N}_{\rm e}$ is either calculated according

to the Kavassalis–Noolandi conjecture $^{28-30}$ in a good solvent or by using the Rubinstein–Colby expression $^{31-33}$ in a marginally good or θ solvent for the polymer backbone as described in the Supporting Information.

In the next section, we perform the data analysis of the concentration dependence of the solution specific viscosity using the following procedure: first, we obtain the parameters B_g and B_{th} from the plateau values of the concentration dependence of normalized specific viscosity $\eta_{\rm sp}/N_{\rm w}(cl^3)^{1/(3\nu-1)}$ with the scaling exponents $\nu = 0.588$ and 0.5, respectively. Second, using values of the B-parameters, we calculate the crossover concentrations c_{th} and c^{**} (eqs 7 and 8), along with the Kuhn length and excluded volume (eqs 9a and 9b). Next, we evaluate the concentration dependence of the number of repeat units g per correlation length (eq 5b) in different solution regimes (Figure 1). Finally, we plot the specific viscosity as a function of the number of correlation blobs per chain $N_{\rm w}/g$ and extract the packing number \tilde{P}_e —the number of overlapping strands of correlation blobs per confining tube diameter-and use it to calculate the concentration dependence of N_e in different ionic liquids.

DATA ANALYSIS

Herein, we apply our method to ionic liquid solutions of cellulose, $^{34-41}$ PEO, 42,43 PMMA, 42 and P(AN-co-IA). 44 The repeat unit chemical structures of these polymers are shown in Figure 2. The cations studied are 1-allyl-3-methylimidazolium (AMIm), 1-ethyl-3-methylimidazolium (EMIm), and 1-butyl-3-methylimidazolium (BMIm), and the anions studied are formate (COOH), chloride (Cl), methylphosphonate [P-(OCH_3)(H)O_2], acetate (Ac), bis(trifluoromethylsulfonyl)-imide (TFSI), hexafluorophosphate (PF_6), and tetrafluoroborate (BF_4) (see Figure 2 for chemical structures). These

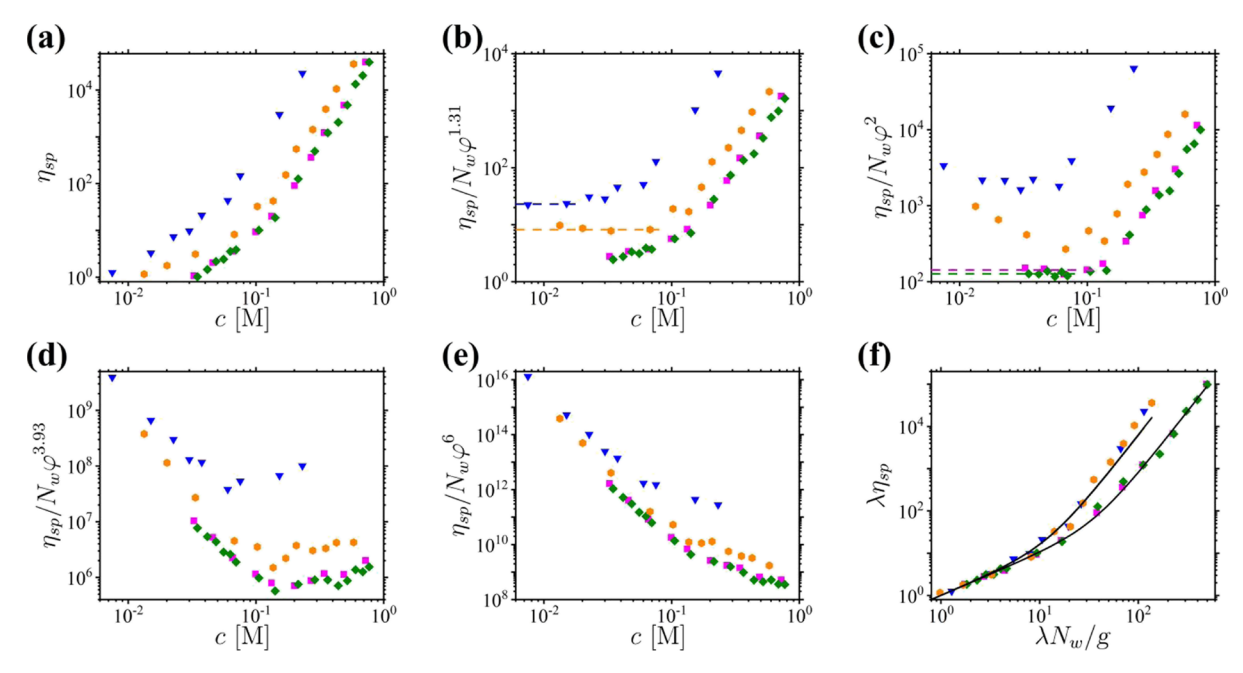


Figure 3. Dependence of solution specific viscosity $\eta_{sp} = (\eta - \eta_s)/\eta_s$ (a), $\eta_{sp}/N_w \varphi^{1.31}$ (b), $\eta_{sp}/N_w \varphi^2$ (c), $\eta_{sp}/N_w \varphi^{3.93}$ (d), and $\eta_{sp}/N_w \varphi^6$ (e) on concentration c in moles of repeat units per liter of the solvent for the solutions of cellulose with the weight-average degree of polymerization $N_w = 741$ in [EMIm][P(OCH₃)(H)O₂] (blue inverted triangles), [BMIm][Cl] (orange hexagons), [AMIm][COOH] (pink squares), and [EMIm][Ac] (green rhombs) at 298 K. (f) Dependence of normalized solution specific viscosity on the normalized number of blobs per chain $\lambda N_w/g$. The solid lines are the best fits for eq S2. The rescaling factor λ is given by eq S4 for [AMIm][COOH] and [EMIm][Ac] solutions and by eq S5 for [BMIm][Cl] and [EMIm][P(OCH₃)(H)O₂]. Dimensionless concentration $\varphi = cl^3$.

Table 1. Summary of Parameters

system	symbol	T [K]	$N_{ m w}$	<i>l</i> [nm]	B_{g}	B_{th}	c* [M]	c _{th} [M]	c** [M]	$g_{ m th}$	<i>b</i> [nm]	v [nm³]	$c_{ m th}b^3$	\widetilde{P}_e
Poly(ethylene oxide), [BMIm][TFSI] 42	•	298	22318	0.338	1.19		0.034							3.5
	•	353			1.12		0.029							3.3
Poly(ethylene oxide), [BMIm][PF ₆] ⁴²	•	298 22318 9000			1.43	0.65	0.059	0.145	7.91	6944	0.79	0.0017	0.04	
	0		0.338	1.43	0.03	0.12	0.143	7.91	0944	0.79	0.0017	0.04	11.9	
	•	353	22318		1.44	0.65	0.061	0.137	7.87	7668	0.79	0.0016	0.04	
Poly(ethylene oxide), [BMIm][BF ₄] 42	•	353	22318	0.338	1.53	0.80 ^d	0.074	0.526	17.30	1706	0.53	0.0019	0.05	7.6
Poly(ethylene oxide), (aq) 42	0	298	22318	0.338	1.11		0.028							3.9
Poly(ethylene oxide), (aq) ^b			9091				0.057							
	∇	293 227	22727	0.338	1.12	0.62	0.028	0.35	6.30	846	0.88	0.0056	0.15	7.2
			90909				0.0098							
Cellulose, [AMIm][COOH] 36	•	298	741	0.54		0.44	0.033		0.39		2.82			6.1
Cellulose, [AMIm][Cl] 38	•	303	220 a	0.54	0.40		0.011							3.0
Cellulose, [EMIm][P(OCH ₃) (H)O ₂] ³⁹		298	741	0.54	0.45		0.0062	•••••		•••••				3.6
Cellulose, [EMIm][Ac] 41	•	298	741	0.54	•••••	0.45	0.034		0.42		2.71			6.1
SSP Cellulose, [EMIm][Ac] ³⁴	•	293	373	0.54	0.80		0.028	•••••		•••••				3.2
	•				0.90		0.040							
Cellulose, [BMIm][Cl] 37	•	298	741	0.54	0.59		0.014	•••••		•••••				3.6
Cellulose, [BMIm][Ac] 40	*	301	780	0.54	0.58	0.34	0.013	0.020	0.14	416	4.68	0.20	1.25	8.2
	*	303			0.58	0.34	0.013	0.021	0.14	416	4.61	0.19	1.22	
Cellulose, [BMIm][Ac] ⁴⁰	*	318	780 0.5			0.35	0.016		0.15		4.52			
	*	333		0.54		0.35	0.016		0.16		4.37			8.3
	*	343				0.36	0.018		0.19		4.06			
Sodium carboxymethyl cellulose, (aq) c		293	811	0.54	0.40	0.25	0.0041	0.01	0.04	243	8.74	0.66	4.17	9.6
Sodium carboxymethyl cellulose, (aq) b		298	889	0.54	0.48	0.30	0.0065	0.02	0.09	215	6.00	0.40	2.56	9.5
Hydroxypropyl methyl cellulose, (aq) ^c	_	293	2281	0.54	0.43		0.0023	•••••						3.0
Methyl cellulose, (aq) ^c		293	1200	0.54	0.43		0.0038			•••••				3.4
Hydroxypropyl cellulose, (aq) ^c			465		0.50		0.0122			•••••				3.4
		298	1703	0.54	0.49		0.0041							2.9
	_		6361		0.51		0.0017							2.7
Hydroxyethyl cellulose, (aq) c		298	1963	0.54		0.23	0.0030	•••••	0.03	•••••	9.91			9.7
Poly(methyl methacrylate), [BMIm][TFSI] 42		298		0.255	0.92	0.47	0.068	0.214	4.71	2228	1.18	0.0035	0.21	9.9
	_	353	9950		0.86	0.44	0.056	0.195	3.81	1950	1.31	0.0033	0.26	
Poly(acrylonitrile-co-itaconic acid), [BMIm][Cl] 44	-	353	1532	0.255	0.71		0.13		2.01	2.00	2.01			3.7

^aThe viscosity-average degree of polymerization. ^bResults previously obtained in ref 16. ^cResults previously obtained in ref 19. ^dThe B_{th} value determined from B_g and c_{th} . An average repeat unit for molecular weight for P(AN-co-IA) is calculated to be 56.16 g/mol given the ratio of acrylonitrile to itaconic acid from ref 44. The values of c^* , c_{th} , and c^* are obtained from eqs 6, 7, and 8, respectively. The values of g_{th} are calculated using eq 5b with $c = c_{th}$. The values of b and b are calculated using eqs 9a and 9b, respectively.

systems are compared to aqueous solutions of PEO^{43} and cellulose derivatives. $^{45-48}$

Figure 3 illustrates an application of the scaling approach to solutions of cellulose with $N_{\rm w} = 741$ in [EMIm][P(OCH₃)-

(H)O₂],³⁹ [BMIm][Cl],³⁷ [AMIm][COOH],³⁶ and [EMIm]-[Ac]⁴¹ at 298 K. Figure 3a shows the original data for solution specific viscosity as a function of repeat unit concentration. Note that we only use data with concentrations less than 10%

of the bulk density of the repeat units, eliminating the need for corrections accounting for changes in the solvent packing around the polymer backbone. First, we determine values of the $B_{\rm g}$ -parameter by plotting the normalized viscosity $\eta_{\rm sp}/N_{\rm w}\varphi^{1.31}$ in Figure 3b. The plateaus at lower concentrations are used to calculate the values of the $B_{\rm g}$ -parameters as $B_{\rm g}=C_{\rm p}^{1/3-\nu}$ (eq 11) using $\nu=0.588$. Here, plateaus are only observed in solutions of [EMIm][P(OCH_3)(H)O_2] ($C_{\rm p}=22.94$) and [BMIm][CI] ($C_{\rm p}=8.20$), resulting in $B_{\rm g}=0.45$ and 0.59, respectively.

Figure 3c shows the solution specific viscosity normalized by $N_{\rm w} \varphi^{\rm I/(3\nu-1)} = N_{\rm w} \varphi^2$ (where $\nu = 0.5$). This normalization should allow us to determine the crossover concentration for the thermal blob overlap regime, $c_{\rm th}$. To make sure that the location of this crossover concentration is not influenced by the crossover to the semidilute entangled solution regime, we plot the concentration dependence of $\eta_{\rm sp}/N_{\rm w}\varphi^{3.93}$ in Figure 3d. For the solutions of cellulose in [BMIm][Cl] and [EMIm]-[P(OCH₃)(H)O₂], the normalized solution specific viscosity $\eta_{\rm sp}/N_{\rm w}\varphi^{3.93}$ plateaus at higher concentrations, indicating that the deviation from the plateau in Figure 3b points to the onset of entanglements. This makes the determination of the crossover concentration c_{th} and parameter B_{th} impossible. However, for cellulose in [AMIm][COOH] and [EMIm][Ac], there are clear plateaus in Figure 3c ($C_p = 141.95$ and 126.80, respectively) and none in Figure 3d or b, which indicates that these are θ solvents for cellulose. This gives the $B_{\rm th}$ for cellulose to be 0.44 in [AMIm][COOH] and 0.45 in [EMIm][Ac]. These values are close to those of cellulose derivatives in aqueous solutions determined previously (between 0.23 and $0.30).^{16,19}$

The thermal blob overlap concentration $c_{\rm th}$ is obtained from eq 7 by using the values of $B_{\rm g}$ and $B_{\rm th}$. For the solutions of cellulose in [AMIm][COOH] and [EMim][Ac], we can confirm that the thermal blobs overlap at high repeat unit concentrations because the normalized solution specific viscosity $\eta_{\rm sp}/N_{\rm w} \varphi^6$ (Figure 3e) plateaus in this solution regime.

Finally, Figure 3f shows the dependence of solution specific viscosity on the number of correlation blobs per chain. Because we cannot calculate the crossover concentration $c_{\rm th}$, we use the Kavassalis–Noolandi conjecture $^{28-30}$ (eqs S1, S2, and S5) for the systems of cellulose in [BMIm][Cl] and [EMIm][P-(OCH₃)(H)O₂] to determine $\tilde{P}_{\rm e}$ and $\tilde{N}_{\rm e}$. This results in the packing number $\tilde{P}_{\rm e}$ for cellulose to be 3.6 in both [BMIm][Cl] and [EMIm][P(OCH₃)(H)O₂]. With the two systems of cellulose in [AMIm][COOH] and [EMIm][Ac], only the value of $B_{\rm th}$ is found, which corresponds to $c_{\rm th} < c^*$. Therefore, using the Rubinstein–Colby conjecture, $^{31-33}$ eqs S1, S2, and S4, we obtain $\tilde{P}_{\rm e}$ to be 6.1 for cellulose in [AMIm][COOH] and [EMIm][Ac]. These values of $\tilde{P}_{\rm e}$ all coincide with the range of $\tilde{P}_{\rm e}$ values of cellulose derivatives in aqueous solutions. 19

Table 1 summarizes the results of our viscosity data analysis for every studied polymer/ionic liquid pair, with corresponding viscosity plots given in the Supporting Information. It should be noted that it is necessary to obtain $B_{\rm th}$ to calculate the crossover concentration c^{**} and Kuhn length b, and both $B_{\rm g}$ and $B_{\rm th}$ are required to evaluate the degree of polymerization of a chain segment inside a thermal blob $g_{\rm th}$, crossover concentration $c_{\rm th}$, and excluded volume ν .

Temperature plays an important role in polymer/solvent affinity. Increasing the temperature increases the crossover concentrations c^* and c^{**} along with parameters $B_{\rm g}$ and $B_{\rm th}$,

which leads to a decrease in the Kuhn length as illustrated in Figure 4 for solutions of cellulose in [BMIm][Ac] (stars) and

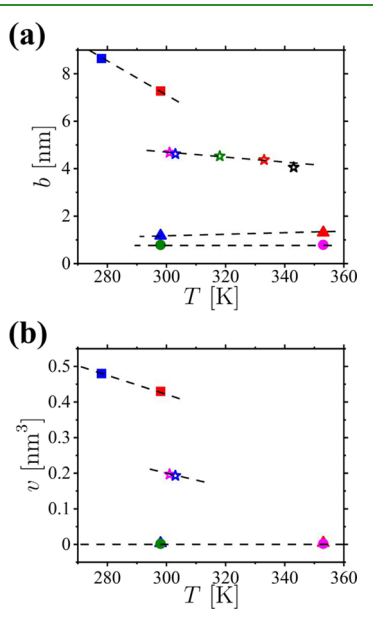


Figure 4. Dependence of the Kuhn length (a) and excluded volume (b) on temperature. Symbol notations are summarized in Table 1. The systems of chitosan in 0.3 M acetic acid at temperatures of 298 K (red square) and 278 K (blue square) from ref 49 are shown for comparison. The dashed lines highlight general trends.

chitosan in 0.3 M acetic acid^{19,49} at temperatures T = 278 K(blue square) and 298 K (red square). For these systems, the excluded volume ν also follows this trend, indicating that these are lower critical point solutions. ²⁵ For the higher temperature data, the good solvent regime was largely inaccessible. With more data at a higher molecular weight, it should be possible to probe this regime and estimate the location of the θ temperature by assuming a linear dependence of ν on 1/T. For solutions of PMMA in [BMIm][TFSI] (triangles) and PEO in [BMIm][PF₆] (circles), the excluded volume is nearly zero at both 298 and 353 K. The Kuhn length for PEO in [BMIm][PF₆] remains constant over the wide temperature range, and for PMMA in [BMIm][TFSI] it increases with increasing temperature. It is worth pointing out that the observed temperature dependence of the B-parameters (Table 1) is consistent with the previous studies of cellulose in ionic liquids. 37,50

It should be noted that our analysis shows a dependence of the chain Kuhn length on the solvent type (Figure 5a). In particular, for polysaccharides, there is a strong solvent effect on the Kuhn length (Table 1), which may be attributed to the solvent-induced changes in the polymer secondary structure. S1-53 For PEO systems, the Kuhn length difference in aqueous solutions and ionic liquids is about 10-15%, which suggests a much weaker effect of the solvent packing on the chain rigidity.

In addition to temperature, the van der Waals radius of different solvent components influences the solvent's ability to pack around the polymer chains (the solvation of the polymer backbone) (Figure 5b). The analysis of PEO in ionic liquids [BMIm][BF₄], [BMIm][PF₆], and [BMIm][TFSI] shows that the B_g -parameter increases as the anion size decreases ⁵⁴ ([BF₄] > [PF₆] > [TFSI]). With further investigations into a wider

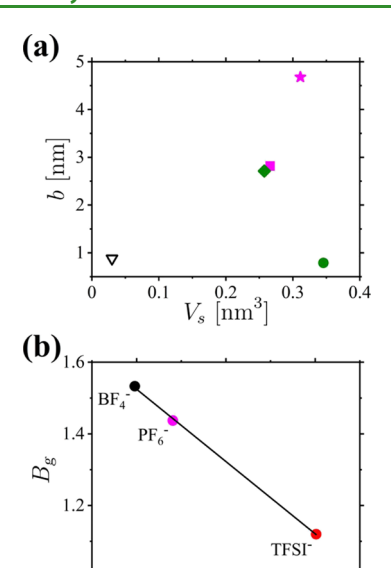


Figure 5. (a) Dependence of the Kuhn length on the excluded volume of solvent molecules for PEO (open triangle and filled green circle) and cellulose (star, rhomb, and square) systems. (b) Dependence of $B_{\rm g}$ of ionic liquid solutions of PEO with [BMIm] cations and anions [BF₄] (black), [PF₆] (pink), and [TFSI] (red) at 353 K on the van der Waals volume of the anions. The line represents the best fit of $B_{\rm g} = mV_{\rm vdw} + B_{\rm g0}$ with $m = -4.04~{\rm nm}^{-3}$ and $B_{\rm g0} = 1.73$. Van der Waals volume data from ref 50.

0.1

 $V_{vdw} [\mathrm{nm}^3]$

0.15

0.05

variety of polymers, cations, and temperatures, a trend could be established in the spirit of the Hofmeister series for ionic liquids. $^{20-24}$

CONCLUSIONS

We have applied a scaling-based approach to describe the solution properties of polymers in ionic liquids. This has allowed us to obtain the values of interaction parameters describing chain statistics at different length scales, including chain Kuhn length and excluded volume from the analysis of the concentration dependence of the specific viscosity (see Figure 3). By applying this approach to polymer solutions where the crossover to the solution regime of overlapping thermal blobs is located within the studied concentration range, we have shown that the Kuhn length and excluded volume are both functions of solvent type and temperature, as summarized in Table 1 and illustrated in Figures 4 and 5. Among the studied set of ionic liquids, we only have examples of lower critical point solutions for which the polymer's second virial coefficient decreases with increasing temperature. ^{25,55}

Furthermore, the strength of the developed framework is that it allows one to determine c^{**} and estimate the polymer Kuhn length in different solvents just from viscosity data analysis without the need for scattering experiments.

Using interaction parameters summarized in Table 1, we can construct a universal diagram of different solution regimes of polymers in ionic liquids. This is shown in Figure 6 which represents different solutions of polymers in ionic liquids in terms of dimensionless excluded volume $v/bl^2 = c_{\rm th}/c^{**}$ (eq 9b) and normalized concentration c/c^{**} . Note that this representation is only possible for the systems for which the crossover concentration $c_{\rm th}$ is located within the studied concentration range and is below the crossover concentration

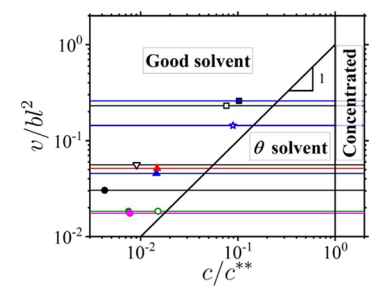


Figure 6. Diagram of different solution regimes in terms of $v/bl^2 = c_{\rm th}/c^{**}$ and c/c^{**} . Symbols show the location of the polymer overlap concentration c^*/c^{**} for studied polymer/ionic liquid systems. Symbol notations are summarized in Table 1.

for the concentrated solution regime ($c_{\rm th} < c^{**}$). For such systems, the dimensionless parameter $v/bl^2 < 1$. It is important to point out that if it is impossible to determine the location of $c_{\rm th}$ from the analysis of the solution viscosity, the polymer is either in a good solvent with $v/bl^2 > 1$, or a θ solvent with $c_{\rm th} < c^*$.

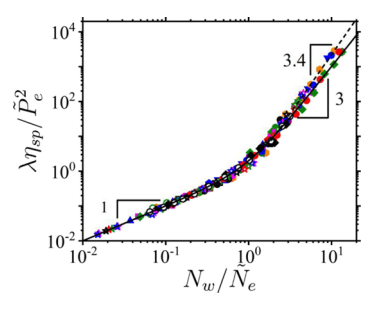


Figure 7. Dependence of normalized specific viscosity $\lambda\eta_{\rm sp}/\tilde{P}_{\rm e}^2$ on the effective number of entanglements per chain $N_{\rm w}/\tilde{N}_{\rm e}$. The solid line is given by eq 11 with $\tilde{N}_{\rm e}=\tilde{P}_{\rm e}^2{\rm g}/\lambda$, and the rescaling factor λ is calculated according to eqs S3–S5. The dashed line corresponds to a slope of 3.4. Symbol notations are summarized in Table 1.

To highlight the universal nature of the polymer solution dynamics, Figure 7 presents all the viscosity data as a function of the number of entanglements per chain in the universal form

$$\lambda \eta_{\rm sp} / \tilde{P}_{\rm e}^{2} = N_{\rm w} / \tilde{N}_{\rm e} [1 + (N_{\rm w} / \tilde{N}_{\rm e})^{2}]$$
(13)

where $\tilde{N}_{\rm e} = \tilde{P}_{\rm e}^2 {\rm g}/\lambda$ and the rescaling factor λ is given by eqs S3–S5, depending on the solvent quality for the polymer backbone. There are two scaling regimes in the dependence of normalized viscosity on the number of entangled strands per chain: the Rouse regime with $\eta_{\rm sp} \sim N_{\rm w}/\tilde{N}_{\rm e}$ and the entangled solution regime, $\eta_{\rm sp} \sim (N_{\rm w}/N_{\rm e})^3$. Note that there is some deviation from this predicted behavior in the dependence of $\eta_{\rm sp} \sim (N_{\rm w}/\tilde{N}_{\rm e})^{3.4}$, which can be explained by tube fluctuations. ^{25,58} The good collapse of the data provides further validation of the scaling-based technique.

Lastly, we hope that the simplicity of our approach will encourage further studies of the solution properties of polymers in ionic liquids and will help with the elucidation of the effect of anion/cation pairs on polymer solubility.

ASSOCIATED CONTENT

5 Supporting Information

The Supporting Information is available free of charge at https://pubs.acs.org/doi/10.1021/acsapm.1c01814.

Calculations of $\tilde{N}_{\rm e}$ and data analysis (PDF)

AUTHOR INFORMATION

Corresponding Author

Andrey V. Dobrynin — Department of Chemistry, University of North Carolina, Chapel Hill, North Carolina 27599, United States; orcid.org/0000-0002-6484-7409; Email: avd@email.unc.edu

Authors

Ryan Sayko — Department of Chemistry, University of North Carolina, Chapel Hill, North Carolina 27599, United States; orcid.org/0000-0002-5986-4829

Michael Jacobs — Department of Chemistry, University of North Carolina, Chapel Hill, North Carolina 27599, United States; orcid.org/0000-0002-7255-3451

Complete contact information is available at: https://pubs.acs.org/10.1021/acsapm.1c01814

Notes

The authors declare no competing financial interest.

ACKNOWLEDGMENTS

This work was supported by the National Science Foundation under the grant DMREF-2049518.

REFERENCES

- (1) Forsyth, S. A.; Pringle, J. M.; MacFarlane, D. R. Ionic Liquids: An Overview. *Aust. J. Chem.* **2004**, *57*, 113–119.
- (2) Curreri, A. M.; Mitragotri, S.; Tanner, E. E. L. Recent Advances in Ionic Liquids in Biomedicine. *Adv. Sci.* **2021**, *8*, 2004819.
- (3) Pinkert, A.; Marsh, K. N.; Pang, S.; Staiger, M. P. Ionic Liquids and Their Interaction with Cellulose. *Chem. Rev.* **2009**, *109*, *6712*–6728.
- (4) Singh, S. K.; Savoy, A. W. Ionic liquids synthesis and applications: An overview. J. Mol. Liq. 2020, 297, 112038.
- (5) Holbrey, J. D.; Seddon, K. R. Ionic Liquids. *Clean Prod. Process.* **1999**, *1*, 223–236.
- (6) Turner, E. A.; Pye, C. C.; Singer, R. D. Use of ab Initio Calculations toward the Rational Design of Room Temperature Ionic Liquids. *J. Phys. Chem. A* **2003**, *107*, 2277–2288.
- (7) Xu, W.; Cooper, E. I.; Angell, C. A. Ionic Liquids: Ion Mobilities, Glass Temperatures, and Fragilities. *J. Phys. Chem. B* **2003**, *107*, 6170–6178.
- (8) Eike, D. M.; Brennecke, J. F.; Maginn, E. J. Predicting melting points of quaternary ammonium ionic liquids. *Green Chem.* **2003**, *5*, 323–328.
- (9) Gericke, M.; Fardim, P.; Heinze, T. Ionic Liquids—Promising but Challenging Solvents for Homogeneous Derivatization of Cellulose. *Molecules* **2012**, *17*, 7458–7502.
- (10) Liu, Z.; Wang, H.; Li, Z.; Lu, X.; Zhang, X.; Zhang, S.; Zhou, K. Characterization of the regenerated cellulose films in ionic liquids and rheological properties of the solutions. *Mater. Chem. Phys.* **2011**, *128*, 220–227.
- (11) Lu, B.; Xu, A.; Wang, J. Cation does matter: how cationic structure affects the dissolution of cellulose in ionic liquids. *Green Chem.* **2014**, *16*, 1326–1335.
- (12) Mondal, J.; Choi, E.; Yethiraj, A. Atomistic Simulations of Poly(ethylene oxide) in Water and an Ionic Liquid at Room Temperature. *Macromolecules* **2014**, *47*, 438–446.

- (13) Zahn, S.; Uhlig, F.; Thar, J.; Spickermann, C.; Kirchner, B. Intermolecular Forces in an Ionic Liquid ([Mmim][Cl]) versus Those in a Typical Salt (NaCl). *Angew. Chem., Int. Ed.* **2008**, 47, 3639–3641.
- (14) Rogers, R. D.; Seddon, K. R. Ionic Liquids-Solvents of the Future? *Science* **2003**, *302*, 792–793.
- (15) Greer, A. J.; Jacquemin, J.; Hardacre, C. Industrial Applications of Ionic Liquids. *Molecules* **2020**, *25*, 5207.
- (16) Dobrynin, A. V.; Jacobs, M.; Sayko, R. Scaling of Polymer Solutions as a Quantitative Tool. *Macromolecules* **2021**, *54*, 2288–2295
- (17) Dobrynin, A. V.; Jacobs, M. When Do Polyelectrolytes Entangle? *Macromolecules* **2021**, *54*, 1859–1869.
- (18) Jacobs, M.; Lopez, C. G.; Dobrynin, A. V. Quantifying the Effect of Multivalent Ions in Polyelectrolyte Solutions. *Macromolecules* **2021**, *54*, 9577–9586.
- (19) Sayko, R.; Jacobs, M.; Dobrynin, A. V. Quantifying Properties of Polysaccharide Solutions. ACS Polym. Au 2021, 1, 196–205.
- (20) Lo Nostro, P.; Ninham, B. W. Hofmeister Phenomena: An Update on Ion Specificity in Biology. *Chem. Rev.* **2012**, *112*, 2286–2322.
- (21) Hofmeister, F. Zur Lehre von der Wirkung der Salze. Naunyn-Schmiedeberg's Arch. Pharmacol 1888, 25, 1–30.
- (22) Kunz, W.; Henle, J.; Ninham, B. W. "Zur Lehre von der Wirkung der Salze" (about the science of the effect of salts): Franz Hofmeister's historical papers. *Curr. Opin. Colloid Interface Sci.* **2004**, *9*, 19–37.
- (23) Moghaddam, S. Z.; Thormann, E. The Hofmeister series: Specific ion effects in aqueous polymer solutions. *J. Colloid Interface Sci.* **2019**, *555*, 615–635.
- (24) Schwierz, N.; Horinek, D.; Sivan, U.; Netz, R. R. Reversed Hofmeister series—The rule rather than the exception. *Curr. Opin. Colloid Interface Sci.* **2016**, 23, 10–18.
- (25) Rubinstein, M.; Colby, R. H. Polymer Physics; Oxford University Press: Oxford, 2007.
- (26) De Gennes, P. G. Dynamics of Entangled Polymer Solutions. I. The Rouse Model. *Macromolecules* **1976**, *9*, 587–593.
- (27) De Gennes, P. G. Dynamics of Entangled Polymer Solutions. II. Inclusion of Hydrodynamic Interactions. *Macromolecules* **1976**, *9*, 594–598.
- (28) Kavassalis, T. A.; Noolandi, J. New View of Entanglements in Dense Polymer Systems. *Phys. Rev. Lett.* **1987**, *59*, 2674–2677.
- (29) Kavassalis, T. A.; Noolandi, J. A new theory of entanglements and dynamics in dense polymer systems. *Macromolecules* **1988**, *21*, 2869–2879.
- (30) Kavassalis, T. A.; Noolandi, J. Entanglement scaling in polymer melts and solutions. *Macromolecules* **1989**, *22*, 2709–2720.
- (31) Colby, R. H.; Rubinstein, M. Two-parameter scaling for polymers in Θ solvents. *Macromolecules* **1990**, 23, 2753–2757.
- (32) Heo, Y.; Larson, R. G. Universal Scaling of Linear and Nonlinear Rheological Properties of Semidilute and Concentrated Polymer Solutions. *Macromolecules* **2008**, *41*, 8903–8915.
- (33) Milner, S. T. Predicting the Tube Diameter in Melts and Solutions. *Macromolecules* **2005**, *38*, 4929–4939.
- (34) Gericke, M.; Schlufter, K.; Liebert, T.; Heinze, T.; Budtova, T. Rheological Properties of Cellulose/Ionic Liquid Solutions: From Dilute to Concentrated States. *Biomacromolecules* **2009**, *10*, 1188–1194.
- (35) Sescousse, R.; Le, K. A.; Ries, M. E.; Budtova, T. Viscosity of Cellulose–Imidazolium-Based Ionic Liquid Solutions. *J. Phys. Chem. B* **2010**, *114*, 7222–7228.
- (36) Lu, F.; Wang, L.; Ji, X.; Cheng, B.; Song, J.; Gou, X. Flow behavior and linear viscoelasticity of cellulose 1-allyl-3-methylimidazolium formate solutions. *Carbohydr. Polym.* **2014**, *99*, 132–139.
- (37) Chen, X.; Zhang, Y.; Wang, H.; Wang, S.-W.; Liang, S.; Colby, R. H. Solution rheology of cellulose in 1-butyl-3-methyl imidazolium chloride. *J. Rheol.* **2011**, *55*, 485–494.
- (38) Kuang, Q.-L.; Zhao, J.-C.; Niu, Y.-H.; Zhang, J.; Wang, Z.-G. Celluloses in an Ionic Liquid: the Rheological Properties of the

Solutions Spanning the Dilute and Semidilute Regimes. J. Phys. Chem. B 2008, 112, 10234-10240.

- (39) Chen, X.; Liang, S.; Wang, S.-W.; Colby, R. H. Linear viscoelastic response and steady shear viscosity of native cellulose in 1-ethyl-3-methylimidazolium methylphosphonate. J. Rheol. 2018, 62, 81-87.
- (40) Lefroy, K. S.; Murray, B. S.; Ries, M. E. Rheological and NMR Studies of Cellulose Dissolution in the Ionic Liquid BmimAc. J. Phys. Chem. B 2021, 125, 8205-8218.
- (41) Lu, F.; Song, J.; Cheng, B.-W.; Ji, X.-J.; Wang, L.-J. Viscoelasticity and rheology in the regimes from dilute to concentrated in cellulose 1-ethyl-3-methylimidazolium acetate solutions. Cellulose 2013, 20, 1343-1352.
- (42) Liu, F.; Lv, Y.; Liu, J.; Yan, Z.-C.; Zhang, B.; Zhang, J.; He, J.; Liu, C.-Y. Crystallization and Rheology of Poly(ethylene oxide) in Imidazolium Ionic Liquids. Macromolecules 2016, 49, 6106-6115.
- (43) Ebagninin, K. W.; Benchabane, A.; Bekkour, K. Rheological characterization of poly(ethylene oxide) solutions of different molecular weights. J. Colloid Interface Sci. 2009, 336, 360-367.
- (44) Zhu, X.; Chen, X.; Saba, H.; Zhang, Y.; Wang, H. Linear viscoelasticity of poly(acrylonitrile-co-itaconic acid)/1-butyl-3-methylimidazolium chloride extended from dilute to concentrated solutions. Eur. Polym. J. 2012, 48, 597-603.
- (45) Lopez, C. G. Entanglement of semiflexible polyelectrolytes: Crossover concentrations and entanglement density of sodium carboxymethyl cellulose. J. Rheol. 2020, 64, 191-204.
- (46) Potier, M.; Tea, L.; Benyahia, L.; Nicolai, T.; Renou, F. Viscosity of Aqueous Polysaccharide Solutions and Selected Homogeneous Binary Mixtures. Macromolecules 2020, 53, 10514-10525.
- (47) Lopez, C. G.; Voleske, L.; Richtering, W. Scaling laws of entangled polysaccharides. Carbohydr. Polym. 2020, 234, 115886.
- (48) Castelain, C.; Doublier, J. L.; Lefebvre, J. A study of the viscosity of cellulose derivatives in aqueous solutions. Carbohydr. Polym. 1987, 7, 1-16.
- (49) Desbrieres, J. Viscosity of Semiflexible Chitosan Solutions: Influence of Concentration, Temperature, and Role of Intermolecular Interactions. Biomacromolecules 2002, 3, 342-349.
- (50) Utomo, N. W.; Nazari, B.; Parisi, D.; Colby, R. H. Determination of intrinsic viscosity of native cellulose solutions in ionic liquids. J. Rheol. 2020, 64, 1063-1073.
- (51) Saalwächter, K.; Burchard, W.; Klüfers, P.; Kettenbach, G.; Mayer, P.; Klemm, D.; Dugarmaa, S. Cellulose Solutions in Water Containing Metal Complexes. Macromolecules 2000, 33, 4094-4107.
- (52) Burchard, W. Solubility and Solution Structure of Cellulose Derivatives. Cellulose 2003, 10, 213-225.
- (53) Schulz, L.; Seger, B.; Burchard, W. Structures of cellulose in solution. Macromol. Chem. Phys. 2000, 201, 2008-2022.
- (54) Katsuta, S.; Imai, K.; Kudo, Y.; Takeda, Y.; Seki, H.; Nakakoshi, M. Ion Pair Formation of Alkylimidazolium Ionic Liquids in Dichloromethane. J. Chem. Eng. Data 2008, 53, 1528-1532.
- (55) Eitouni, H. B.; Balsara, N. P. Thermodynamics of Polymer Blends. In Physical Properties of Polymers Handbook; Mark, J. E., Ed.; Springer New York: New York, NY, 2007; pp 339-356.
- (56) Doi, M.; Edwards, S. F. The Theory of Polymer Dynamics; Oxford University Press: New York, 1986.

□ Recommended by ACS

Predicting Phase Behavior of Linear Polymers in Solution Using Machine Learning

Jeffrey G. Ethier, Richard A. Vaia, et al.

MARCH 24 2022 MACROMOLECULES

READ 2

Nonlinear Extensional Rheology of Poly(n-alkyl methacrylate) Melts with a Fixed Number of Kuhn Segments and Entanglements per Chain

Shilong Wu, Quan Chen, et al.

MARCH 22, 2022 ACS MACRO LETTERS

READ **C**

Molecular Weight Dependence of the Viscosity of **Highly Entangled Polyisobutylene**

Timothy C. Ransom, C. Michael Roland, et al.

JULY 03, 2019 MACROMOLECULES

RFAD 17

Structure-Dilute Solution Property Relationships of Comblike Macromolecules in a Good Solvent

Robert J. S. Ivancic, Debra J. Audus, et al.

JANUARY 19, 2022

MACROMOLECULES

READ **C**

Get More Suggestions >